Structure and magnetic order in $La_{1-x}Ca_xMnO_3$ $(0<x\leqslant 0.33)$

Q. Huang
National Institute of Standards and Technology, NIST Center for Neutron Research, Gaithersburg, Maryland 20899 and Materials Research Program, University of Maryland, College Park, Maryland 20742

A. Santoro
National Institute of Standards and Technology, NIST Center for Neutron Research, Gaithersburg, Maryland 20899

J. W. Lynn
National Institute of Standards and Technology, NIST Center for Neutron Research, Gaithersburg, Maryland 20899 and Center for Superconductivity Research, University of Maryland, College Park, Maryland 20742

R. W. Erwin and J. A. Borchers
National Institute of Standards and Technology, NIST Center for Neutron Research, Gaithersburg, Maryland 20899

J. L. Peng, K. Ghosh, and R. L. Greene
Center for Superconductivity Research, University of Maryland, College Park, Maryland 20742
(Received 3 October 1997; revised manuscript received 12 January 1998)

The nuclear and magnetic structures of $La_{1-x}Ca_xMnO_3$ have been studied by neutron powder diffraction methods for the compositions $x=0.06$, 0.15, 0.175, 0.25, and 0.33. At low concentrations of Ca ($x=0.06$) the oxidized sample contains cation vacancies and the structure is ferromagnetic, while in reduced samples all atomic sites are fully occupied and the structure is antiferromagnetic. This result explains the discrepancies found in published phase diagrams. In the samples with compositions $x\geqslant 0.15$, the structural distortions associated with the magnetic and electronic transitions increase with increasing Ca content. These distortions consist mainly of an increase in the tilting of the MnO_6 octahedra and a consequent sharp decrease of the Mn-Mn separations as the system becomes metallic and ferromagnetic. These readjustments of the structure may be responsible for the metallic character of the bonds at the transition from insulating to metallic behavior. The magnetic-field dependence of the lattice parameters, studied in sample $x=0.33$ at two fixed temperatures (270 and 240 K), demonstrates that there is strong coupling between the magnetization and the structural properties in this system. [S0163-1829(98)06329-2]

INTRODUCTION

Rare-earth manganites have the basic perovskite structure and display numerous and complex magnetic and structural transitions, some of which are associated with changes of the nature of the electrical conductivity. Since the magnetic structures of these materials depend on the coupling of Mn^{3+} and Mn^{4+} cations, methods have been devised to vary the relative concentrations of these cations. Lanthanum manganite, of nominal composition $LaMnO_3$, is an insulator at all temperatures and its nuclear and magnetic structures have been reported in various publications[1–5] as having orthorhombic or trigonal symmetry, with ferromagnetic or antiferromagnetic ordering of the Mn spins. In a recent study of the system $La_{3/(3+\delta)}(Mn^{3+}_{(3-6\delta)/(3+\delta)}Mn^{4+}_{6\delta/(3+\delta)})O_3$ (Ref. 6) it was found that the magnetic and structural properties depend critically on the preparation method and consequent oxidation state of the sample. Stoichiometric $LaMnO_3$ is orthorhombic, and below the Néel temperature the magnetic structure consists of ferromagnetic sheets parallel to the a-c plane stacked antiferromagnetically along the b direction. On the other hand, the oxidized phases with concentrations of Mn^{4+} larger than about 10% ($\delta>0.051$) are ferromagnetic and the nuclear structure may have orthorhombic or trigonal-monoclinic symmetry, depending on the relative concentration of Mn^{4+}.

The concentration of Mn^{4+} attainable in the undoped compound is limited, and in order to obtain compositions with more than about 35% of Mn^{4+}, doping with divalent Ca, Ba, or Sr becomes necessary. The system $La_{1-x}Ca_xMnO_3$ has been studied extensively because it offers the possibility of varying the Mn formal valence over the entire range between $+3$ and $+4$, without significant change of the La/Ca size, due to the fact that the ionic radii of La^{3+} (XII) and Ca^{2+} (XII) are almost identical (1.36 and 1.34 Å, respectively).[7]

The first complete phase diagram of the system $La_{1-x}Ca_xMnO_3$ was published by Goodenough,[8] who predicted the existence of five phases, labeled from α to ε, and derived their composition range, their nuclear and magnetic structures, and their conductivity properties from the semicovalent model for the coupling of Mn^{3+} and Mn^{4+}. A phase diagram has been published more recently by Schiffer *et al.*[9] and the results of these two studies are in remarkable agreement, with the exception of the magnetic structure at low concentrations of Ca^{2+}, which is reported as antiferromagnetic in Ref. 8 and as ferromagnetic in Ref. 9. Schiffer *et al.* attributed the discrepancy to a high sensitivity to oxygen

TABLE I. Sample preparation conditions and phase relations for $La_{1-x}Ca_xMnO_3$. As-prepared (AS): sample prepared at 1350 °C in air (2 days); Annealed (AN): The as-prepared sample annealed at 900 °C (5 h) in N_2 with Ti metal as a getter.

Symbol (x condition)	T (K)	Phase	a (Å)	b (Å)	c (Å)	Magnetic properties			
						State	μ_{Mn} (μ_B)	T_C (K)	T_N (K)
0.06-AS[a]	300	*Pnma*	5.4860(2)	7.7648(2)	5.5262(2)				
		$R\bar{3}c$	5.5246(3)		13.3264(6)				
	10	*Pnma*[b]	5.4802(1)	7.7566(2)	5.5178(1)	FM	2.88(2)	~170	
0.06-AN	300	*Pnma*	5.6854(2)	7.7052(3)	5.5361(2)				
	10	*Pnma*	5.6931(2)	7.6694(2)	5.5333(1)	AFM	3.47(3)		~140
0.15-AS	300	*Pnma*	5.4869(2)	7.7612(2)	5.5239(4)				
	10	*Pnma*	5.4835(1)	7.7514(2)	5.5015(1)	FM	2.88(3)	~150	
0.15-AN[c]	300	*Pnma*-I[d]	5.5239(4)	7.8108(6)	5.5260(5)				
		Pnma-II							
	10	*Pnma*-I	5.5213(5)	7.7894(6)	5.5200(8)	FM	1.34(6)		
		Pnma-II				AFM	3.6(1)		
0.175-AS	300	*Pnma*	5.4862(2)	7.7603(3)	5.5072(2)				
	10	*Pnma*	5.4927(3)	7.7495(3)	5.4977(2)	FM	2.96(3)	~175	
0.25-AS	300	*Pnma*	5.4784(3)	7.7394(6)	5.4931(4)				
	10	*Pnma*	5.4676(3)	7.7283(5)	5.4826(4)	FM	3.30(2)	~250	
0.33-AS	300	*Pnma*	5.4654(2)	7.7231(3)	5.4798(2)				
	10	*Pnma*	5.4556(1)	7.7070(2)	5.4693(2)	FM	3.46(2)	~260	

[a] *Pnma* (85 wt %) + $R\bar{3}c$ (15 wt %) at 300 K and *Pnma* (97 wt %) + $R\bar{3}c$ (3 wt %) at 250 K (No rhombohedral phase is observed below 14 K).

[b] Refined composition: $[(La_{0.94}Ca_{0.06})_{0.96}\square_{0.04}][(Mn^{3+}{}_{0.69}Mn^{4+}{}_{0.31})_{0.96}\square_{0.04}]O_3$.

[c] *Pnma*-I (95%) + *Pnma*-II (5%) over the temperature range of the measurements.

[d] Refined composition: $(La_{0.85}Ca_{0.15})(Mn^{3+}{}_{0.93}Mn^{2+}{}_{0.07})(O_{2.89}\square_{0.11})$.

content in samples with $x<0.1$, but no details were given about the structural features responsible for the difference between the two results. A more complex picture of the phase diagram of the Ca-doped manganites has emerged from recent work of Cheong and co-workers.[10] These authors have shown that some physical properties of the system, such as charge ordering, magnetic transition temperatures, etc., show anomalies at $x=N/8$, with $N=1,3,4,5,7$. No structural details are available at the present time to clarify this intriguing behavior.

In the region $0.1<x<0.5$, the ordering of the Mn spins is purely ferromagnetic, and the appearance of magnetic ordering is always accompanied by a transition from insulating to metallic behavior. These transitions are strongly coupled with structural distortions. For example, abrupt decreases in the curves of the lattice parameters versus temperature were observed in $La_{0.75}Ca_{0.25}MnO_3$ by Radaelli *et al.*[11] at the magnetic transition temperature (~240 K), and these sharp anomalies were attributed to both the magnetic ordering and the change in the electronic properties. A similar decrease of the unit-cell volume was found for the composition $x=0.33$ by De Teresa *et al.*[12] when long-range magnetic order sets in at about 260 K. The structural features associated with these lattice distortions were not determined, however, in these publications, and it was this lack of information about the relationship between crystal structure and magnetic and electronic properties that prompted us to undertake a detailed analysis of the crystallography of the system $La_{1-x}Ca_xMnO_3$ in the range of compositions $0<x\leqslant 0.33$. The study of materials with $x>0.33$ is in progress and will be the subject of a subsequent paper.

EXPERIMENTAL

All materials used in this study were prepared by mixing the required quantities of La_2O_3, $MnCO_3$, and $CaCO_3$, using the conditions indicated in Table I. Attempts to anneal in reducing atmosphere samples with a Ca^{2+} concentration greater than 15% were unsuccessful because compounds decompose easily at high Ca content. In what follows, the samples used in this work are indicated with a number equal to the composition x, followed by the letters AS and AN to indicate the ''as-prepared'' and ''annealed'' materials.

The neutron powder diffraction measurements were carried out with the BT-1 high-resolution powder diffractometer at the National Institute of Standards and Technology, using a neutron beam of wavelength $\lambda=1.5396(1)$ Å, produced by a copper (311) monochromator, and collimators with horizontal divergences of 15, 20, and 7 min of arc for the in-pile, monochromatic, and diffracted beams, respectively. The intensities were measured in steps of 0.05° over 2θ angular range 3–165°. For each sample, data were collected at various temperatures in the range 10–300 K to determine the nuclear and magnetic structures and to elucidate the nature of the lattice distortions associated with the magnetic and electronic transitions.

Crystal structure refinements were carried out with the program GSAS,[13] using the following values of the scattering

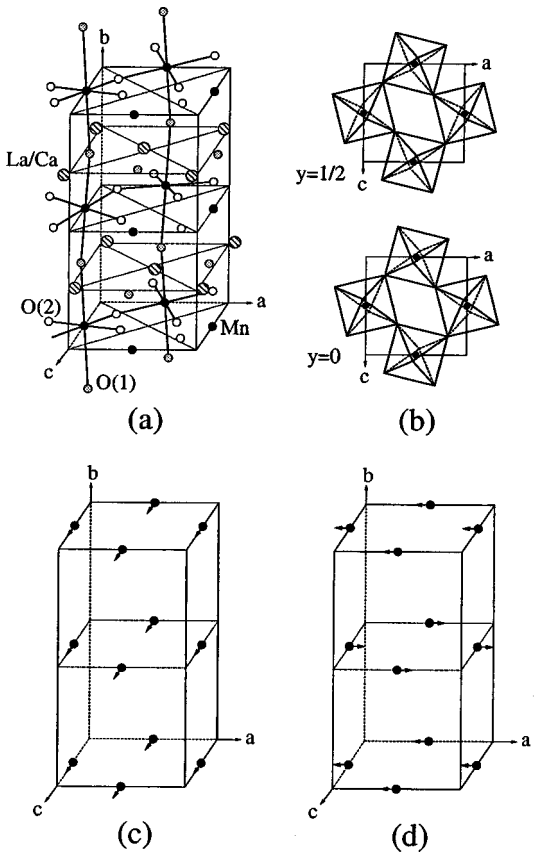

FIG. 1. (a) Schematic representation of the orthorhombic structure of $La_{1-x}Ca_xMnO_3$; (b) Representation of the tilting system of the MnO_6 octahedra; (c) and (d) orientation of the Mn magnetic moments in the ferromagnetic and antiferromagnetic structures, respectively.

amplitudes: $b(\mathrm{La})=0.827$, $b(\mathrm{Mn})=0.344$, $b(\mathrm{Ca})=0.470$, and $b(\mathrm{O})=0.581(\times 10^{-12}\ \mathrm{cm})$. The structural parameters used in the initial stages of the refinements were those obtained in the previous work on the undoped manganites.[6]

The phase composition and the crystal data of each sample are shown in Table I. Tables of the atomic parameters and the relevant bond distances and angles are available with the Physics Auxiliary Publication Service.[14] A schematic representation of the nuclear and magnetic structures of $La_{1-x}Ca_xMnO_3$ is illustrated in Fig. 1.

RESULTS AND DISCUSSION

As shown in Table I, structure and magnetic properties of the compounds in the Ca-doped system are strongly affected by preparation conditions and heat treatments. Some of these materials (such as the orthorhombic phase of sample 0.06-AS and the *Pnma* I phase of 0.15-AN) show the presence of small concentrations of cation or anion vacancies. To circumvent the problem generated by the high correlation of occupancy and thermal parameters, the small departures from the expected stoichiometry were determined in these cases from refinements in which the thermal factors of all atoms were allowed to vary, while the occupancy parameters of the sites under investigation were kept fixed at several values in the range 0.88–1.00. Following previous results,[15] it was assumed that the cation vacancies in sample 0.06-AS occur in equal number on the La/Ca and Mn sites. Figure 2(a) shows that for this sample an increase of the cation site occupancy is accompanied by an increase of the cation thermal factors and by a decrease of the thermal factors of O(1) and O(2). This behavior is typical in these compounds.[6] The correlation between the occupancy factor $n(\mathrm{O2})$ and the thermal parameters of all atoms in sample 0.15-AN is illustrated in Fig. 2(b).

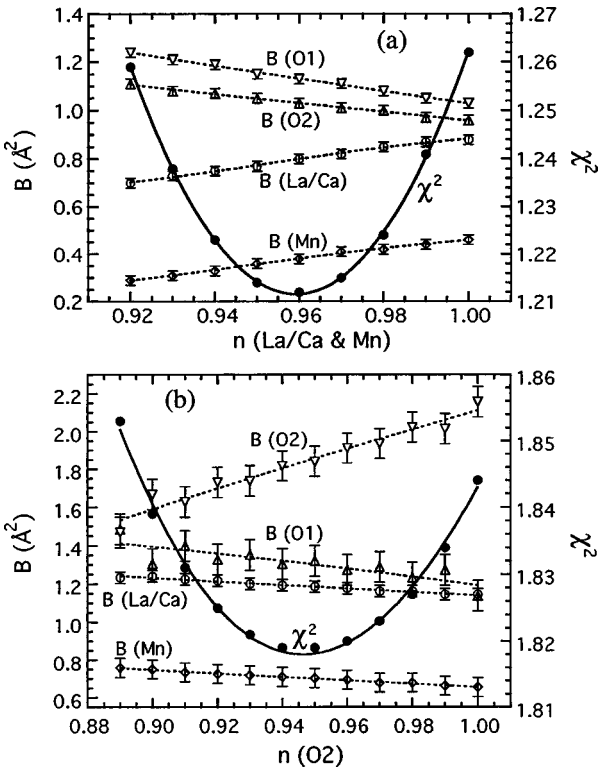

FIG. 2. Plots of temperature factors $B(\mathrm{Å}^2)$ and goodness of fit χ^2 as a function of (a) the occupancy factors of the cations in the case of sample 0.06-AS; and (b) the occupancy factor of the O(2) sites in the case of sample 0.15-AN.

The agreement between observed and calculated intensities, expressed by the goodness of fit χ^2, is also a function of n. The plots of χ^2 versus n have minima corresponding to $n(\mathrm{La/Ca})=n(\mathrm{Mn})\cong 0.96$ and $n(\mathrm{O2})\cong 0.95$ for samples 0.06-AS and 0.15-AN, respectively. The presence of these minima, and the fact that they occur at reasonable values of the thermal factors, are a strong indication that the existence of vacancies in the two samples is real.

The above results show that in doped lanthanum manganites the concentration of Mn^{4+} may be controlled not only by the amount and the valence of the dopant, but also by the possible presence of cationic and/or anionic vacancies. Since the magnetic and electronic properties depend critically from the Mn^{3+}/Mn^{4+} ratio, it is always vital to carefully characterize the materials under study.

A comparison between samples 0.06-AS and 0.06-AN (for both of which $x=0.06$) can illustrate this point. As shown in Table I, in the orthorhombic phase of sample 0.06-AS about 30% of the Mn cations have 4+ valence and, consistent with Goodenough's phase diagram,[8] the magnetic ordering that develops below 170 K [Fig. 3(d)] is purely ferromagnetic. In addition, at this concentration of Mn^{4+} no significant Jahn-Teller effect is observed, and the tilt angle of

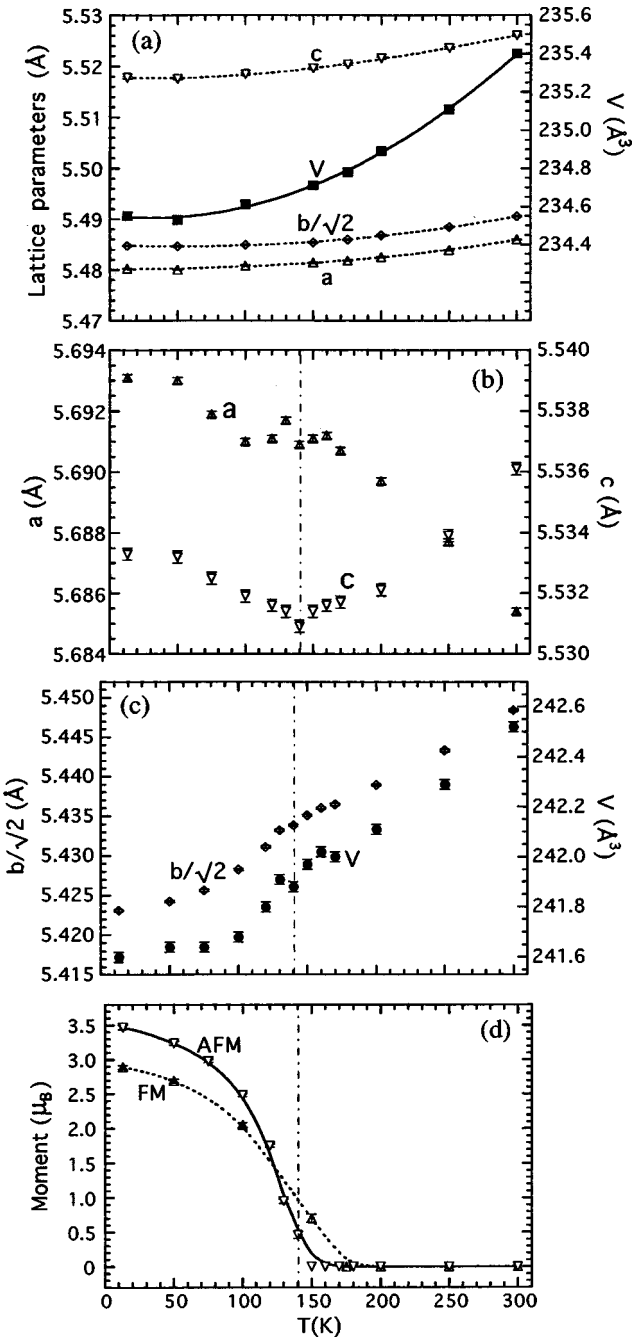

FIG. 3. Variation of lattice parameters and unit cell volume for (a) sample 0.06-AS; (b) and (c) sample 0.06-AN. (d) Magnetization curves for the antiferromagnetic (AFM) and ferromagnetic (FM) structures of samples 0.06-AN and 0.06-AS, respectively.

the MnO_6 octahedra is 9–10°. On the other hand, in the annealed sample 0.06-AN the concentration of Mn^{4+} is only 6% and, in agreement with Goodenough's predictions, the magnetic ordering that develops below 140 K [Fig. 3(d)] is antiferromagnetic (Table I). Further, in this sample the MnO_6 octahedra are significantly distorted by the Jahn-Teller effect and are tilted with a rather large angle of about 12°. The behavior of the lattice parameters of the two samples as a function of temperature is illustrated in Figs. 3(a)–3(c). No anomalies are present in the case of sample 0.06-AS, while for 0.06-AN the *a* parameter has a negative thermal expansion over the entire range of temperatures studied, and the *c*

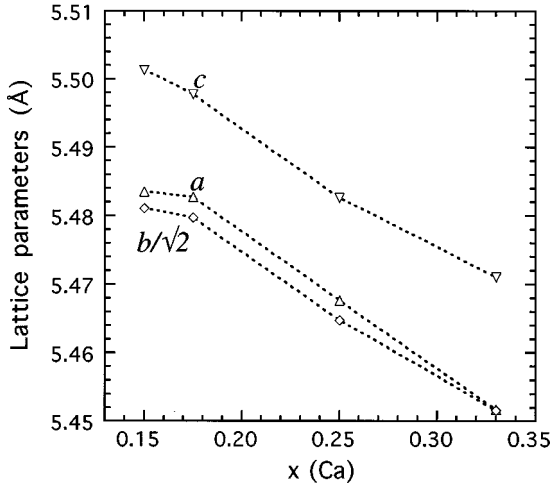

FIG. 4. Variation of the lattice parameters as a function of Ca content *x* for the ''as-prepared'' compositions. The data shown in the figure are for 10 K.

parameter has a positive thermal expansion between 150 and 300 K, and negative below 150 K. These results show that samples with the same concentration of Ca doping may have drastically different magnetic and structural properties, depending on the preparation method and the presence of defects (such as vacancies) in the structure. The above results also explain the discrepancies regarding the magnetic struc-

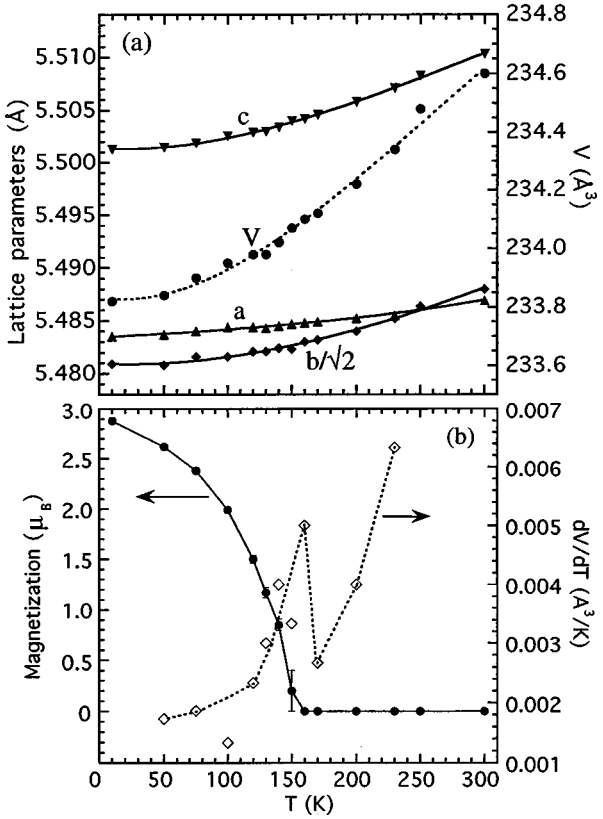

FIG. 5. (a) Lattice parameters and unit-cell volume; and (b) magnetization and $\Delta V/\Delta T$ curves, as a function of temperature for sample 0.15-AS (transition temperature ~150 K). The connecting lines are a guide for the eye.

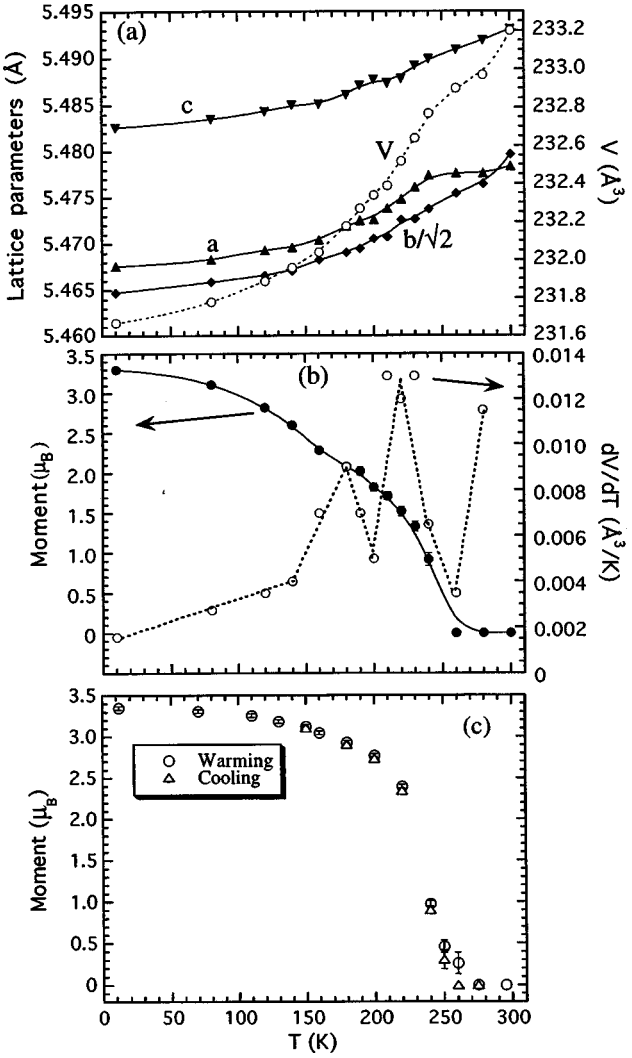

FIG. 6. (a) Lattice parameters and unit-cell volume; (b) magnetization and $\Delta V/\Delta T$ curves as function of temperature for the original sample 0.25-AS (transition temperature is about 240 K) prepared as indicated in Table I; (c) magnetization data for the second sample of the same composition, prepared by annealing the previous sample at 1100 °C four times, and then at 1250 °C and 1350 °C with regrindings between each heat treatment. The connecting lines are a guide for the eye.

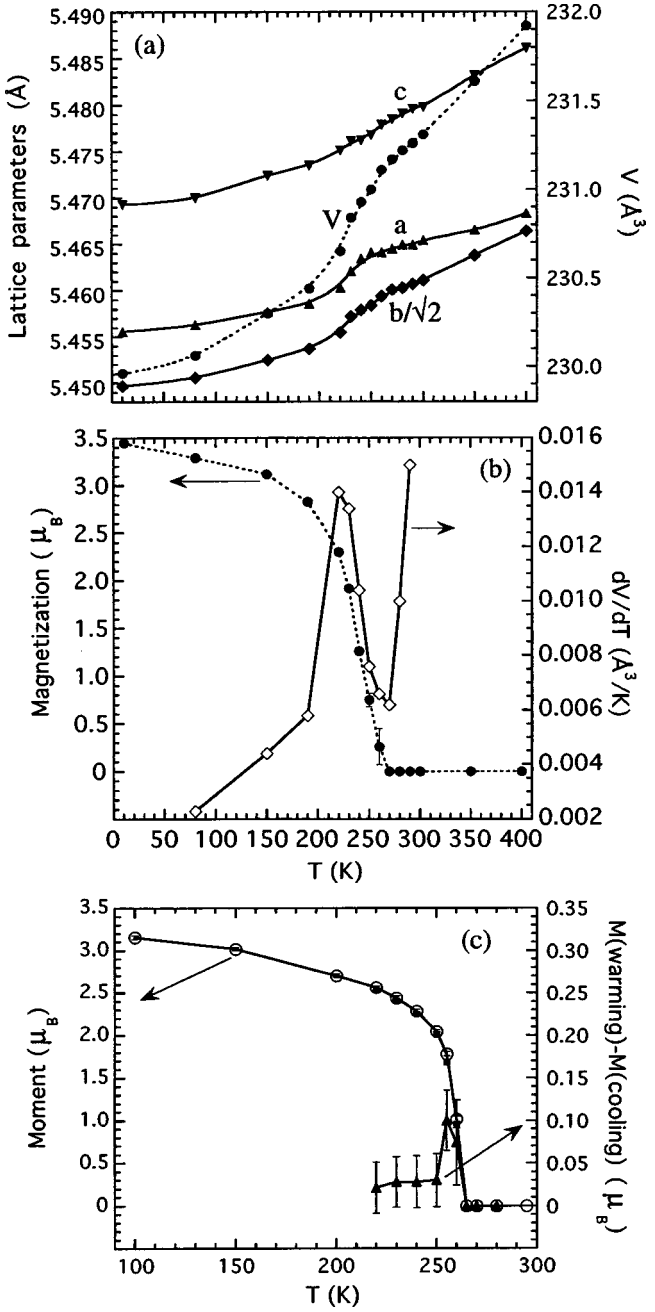

FIG. 7. (a) Lattice parameter and unit-cell volume; (b) magnetization and $\Delta V/\Delta T$ curves as function of temperature for sample 0.33-AS (transition temperature is about 260 K). Some evidence of systematic differences on the magnetization curve on heating and cooling for this composition has been observed. (c) Magnetization curve for a second sample of the same composition [annealed under conditions similar to those used for Fig. 6(c)], showing a very small difference of behavior on heating and cooling.

ture at low concentrations of Ca in the phase diagram determinations reported in Refs. 8 and 9.

A second example showing the effect of different preparation methods on the physical properties of the Ca-doped manganites is illustrated by the magnetization curves of the 0.25-AS samples of Figs. 6(b) and 6(c). The magnetization curve of the sample of Fig. 6(c) does not have any unusual features, while that of Fig. 6(b) shows irregularities at $\sim$220 K and $\sim$180 K. (These features are also observed in the bulk magnetization data). The first of these irregularities is associated with the electronic and magnetic transitions, while the second is intriguing and interesting in itself, especially in view of the work of Cheong and co-workers[10] showing that the phase diagram of the Ca-doped manganites is more complex than thought before. This behavior may in fact be due to an ordering transition involving Mn^{3+} and Mn^{4+} at the 25% composition. Refinements of simple models reflecting this possibility have so far been inconclusive, but further studies on the nature of the 180 K transition are still underway.

Due to the presence of oxygen vacancies, sample 0.15-AN does not contain Mn^{4+} cations in the structure, and for this reason antiferromagnetic behavior would be expected theoretically.[8] Our results, however, show ferromagnetic ordering with a low value of the magnetic moment, which coexists with short-range antiferromagnetic correlations.

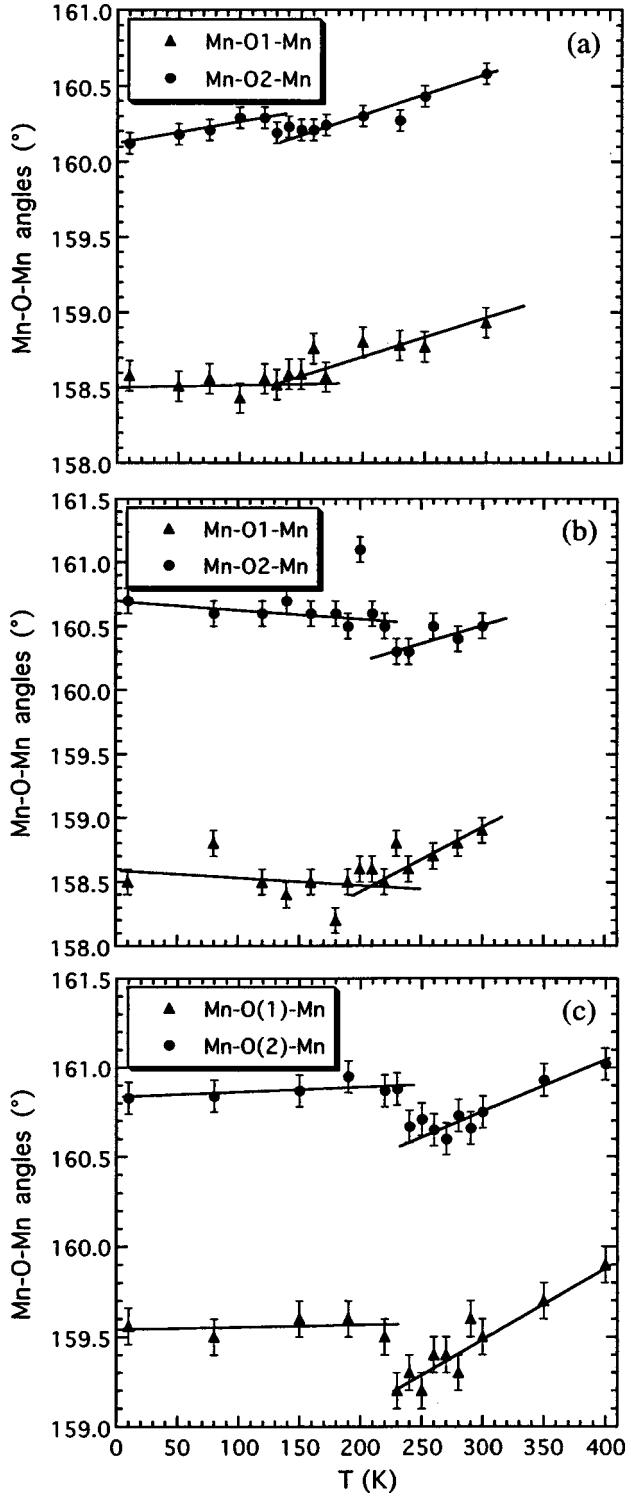

FIG. 8. Plots of tilting angles of the MnO_6 octahedra as a function of temperature for samples (a) 0.15-AS; (b) 0.25-AS; and (c) 0.33-AS.

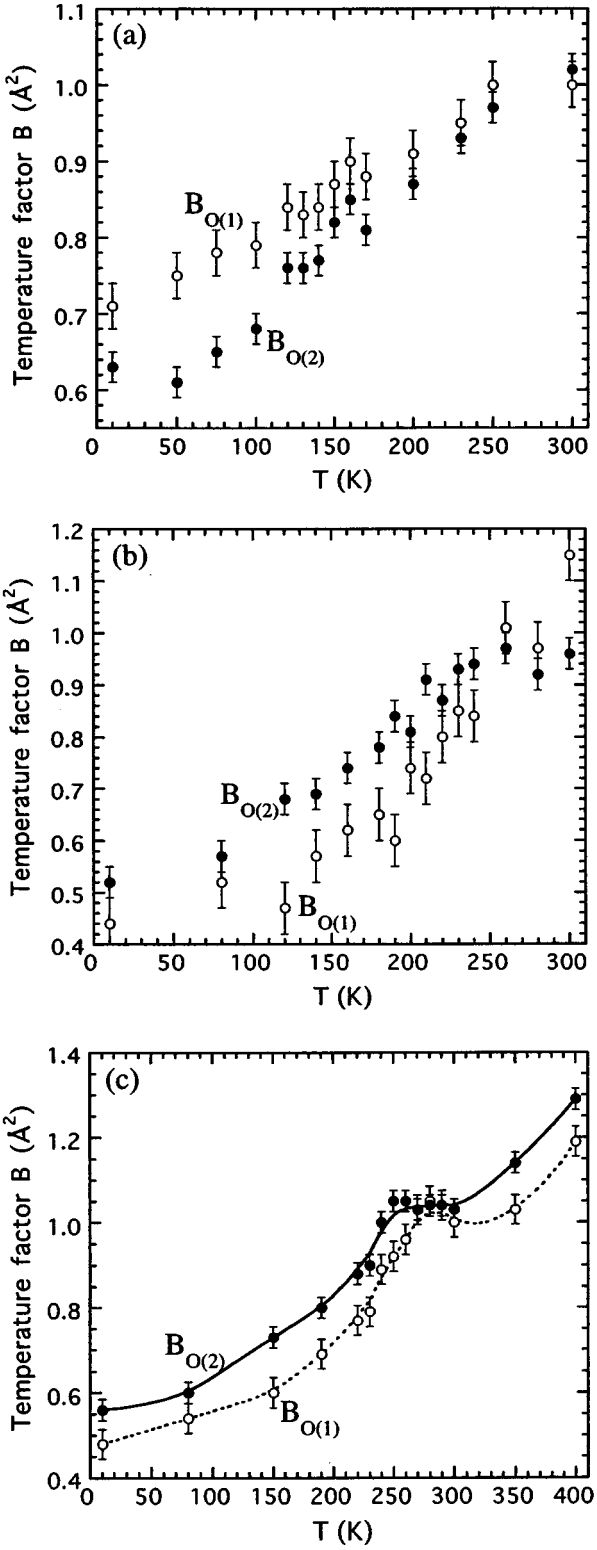

FIG. 9. Plots of the temperature factors of oxygen atoms O(1) and O(2) as a function of temperature for samples (a) 0.15-AS; (b) 0.25-AS; and (c) 0.33-AS.

This departure from the predicted behavior may be caused by the high degree of structural disorder, reflected in the observed high values of the thermal parameters of all atoms in the structure.

The results listed in Table I show that all the ''as-prepared'' samples with $x \geqslant 0.15$ are monophasic and have the same nuclear and ferromagnetic structures. From the refinements it was found that no vacancies of any type are present in these materials and, therefore, the concentration of Mn^{4+} is always equal to that of Ca^{2+}. As indicated in Fig. 4, the lattice parameters decrease for increasing values of x. Since the ionic radii of Ca^{2+} and La^{3+} are practically identical, this result is entirely due to the increasing concentration of Mn^{4+}.

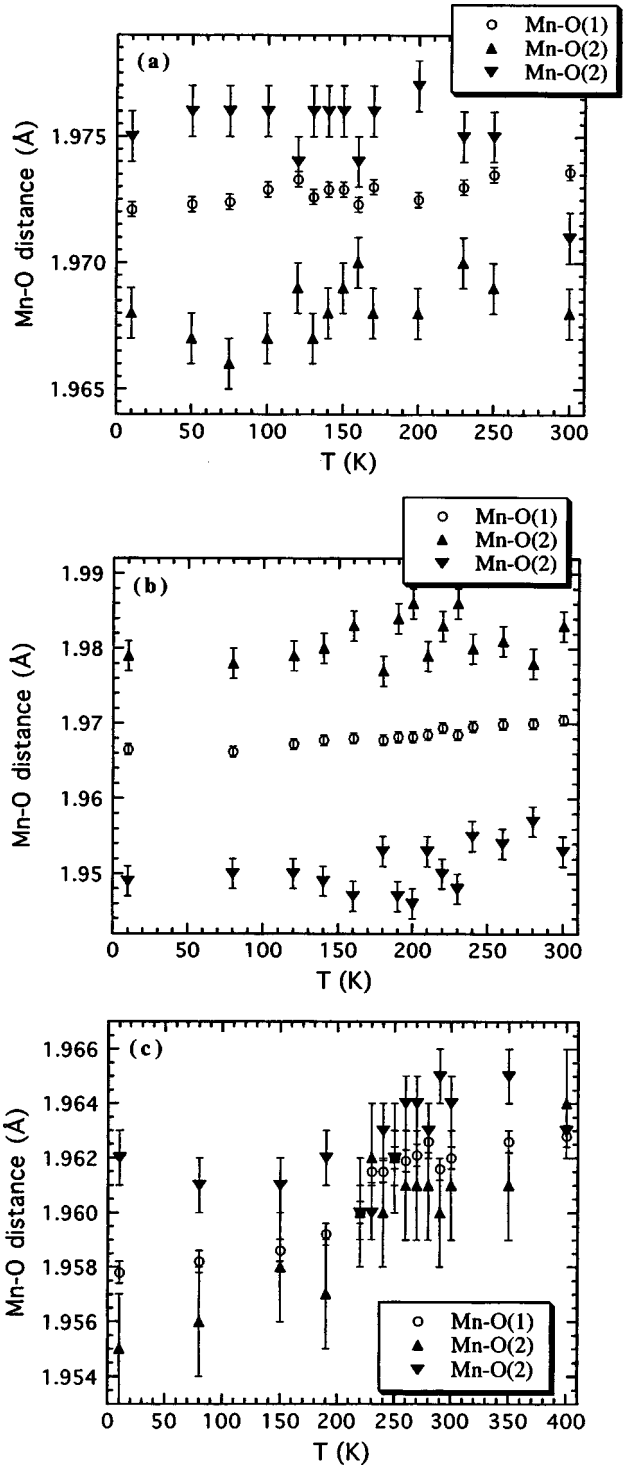

FIG. 10. Variations, as a function of temperature, of the Mn-O distances in samples (a) 0.15-AS; (b) 0.25-AS; and (c) 0.33-AS.

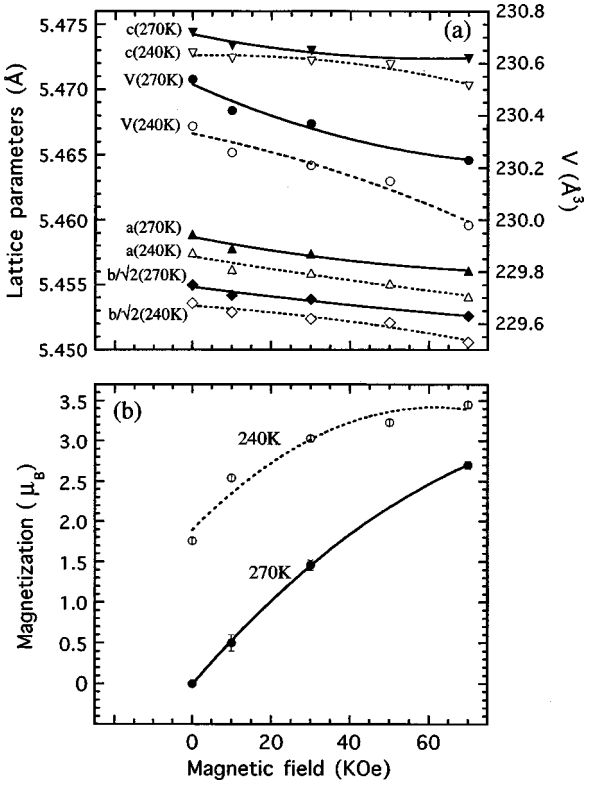

FIG. 11. Variation of (a) lattice parameters and unit-cell volume; and (b) magnetization of sample 0.33-AS as a function of external magnetic field at 270 and 240 K. The curves are a guide for the eye. Error bars for case (a) are smaller than the symbols used in the figure.

The variation of lattice parameters and unit-cell volume as a function of temperature, and the magnetization curves as determined from the neutron refinements, are illustrated in Figs. 5, 6, and 7 for samples 0.15-AS, 0.25-AS, and 0.33-AS, respectively. In agreement with previously published results,[11,12] these plots show that the appearance of long-range ferromagnetic ordering is accompanied by significant structural distortions whose magnitude increases with increasing Ca content [Figs. 5(a), 6(a), and 7(a)]. As indicated in Fig. 8, the tilting angles of the MnO_6 octahedra decrease with decreasing T above the Curie temperature, undergo an abrupt variation at T_c, and remain practically constant for $T<T_c$. This structural readjustment is more pronounced at high Ca concentrations and is associated with anomalously high values of the atomic thermal parameters (especially those of the oxygen atoms) in a range of temperatures around T_c (Fig. 9).

In the range of compositions corresponding to $x>0.1$, these materials display a transition from insulating to metallic behavior at the same temperature T_c at which magnetic ordering occurs.[8,9] This change in the transport properties must be associated with an increase in the metallic nature of the bonds. The data illustrated in Fig. 10 show very little change of the Mn-O separations with temperature, and, in fact, only for sample 0.33-AS is a shortening of these distances noticeable. On the other hand, short Mn-Mn distances, which may be associated with the electronic behavior, are achieved through the previously discussed increase in the tilting of the MnO_6 octahedra. It seems, therefore, that the distortion of the structure is specifically designed to bring about short Mn-Mn separations and that the driving force for the transition has to be found in the electronic behavior of these materials.

The coupling between structure and magnetism at all the compositions analyzed in this study is clearly indicated by the results discussed previously. An additional, dramatic demonstration of this effect is given by the magnetic-field dependence of the lattice parameters illustrated in Fig. 11 for the case of sample 0.33-AS at two fixed temperatures (270

and 240 K). At both temperatures the unit cell of the structure shrinks significantly and continuously with development of spin ordering induced by the external field. This behavior, which is unusual in ferromagnetic systems, shows that the spin ordering is strongly coupled to the lattice.

In conclusion, we have been able to show that preparation conditions have a significant effect on the structural and magnetic properties of Ca-doped lanthanum manganites, and that published inconsistencies about the magnetic structure at low concentrations of Ca^{2+} can be explained by the presence or absence of cationic vacancies in the structure. We have also shown that the main structural features associated with the magnetic and electronic transitions are related to a rearrangement in the tilting of the MnO_6 octahedra, and that there is a strong coupling between magnetism and structural distortions.

ACKNOWLEDGMENTS

We would like to thank S. W. Cheong for helpful discussions. Work at the University of Maryland was supported in part by the MRSEC program of the NSF, DMR 96-32521.

[1] E. O. Wollan and W. C. Koehler, Phys. Rev. **100**, 545 (1955).
[2] H. L. Yakel, Jr., Acta Crystallogr. **8**, 394 (1955).
[3] J. B. A. A. Elemans, B. Van Laar, K. R. Van Der Veen, and B. O. Loopstra, J. Solid State Chem. **3**, 238 (1971).
[4] B. C. Tofield and W. R. Scott, J. Solid State Chem. **10**, 183 (1974).
[5] R. J. H. Voorhoeve, J. P. Remeika, L. E. Trimble, A. S. Cooper, F. J. DiSalvo, and P. K. Gallagher, J. Solid State Chem. **14**, 395 (1975).
[6] Q. Huang, A. Santoro, J. W. Lynn, R. W. Erwin, J. A. Borchers, J. L. Peng, and R. L. Greene, Phys. Rev. B **55**, 14 987 (1997).
[7] R. D. Shannon, Acta Crystallogr., Sect. A: Cryst. Phys., Diffr., Theor. Gen. Crystallogr. **32**, 751 (1976).
[8] J. B. Goodenough, Phys. Rev. **100**, 564 (1955).
[9] P. Schiffer, A. P. Ramirez, W. Bao, and S-W. Cheong, Phys. Rev. Lett. **75**, 3336 (1995).
[10] S-W. Cheong, C. M. Lopez, and H. Y. Hwang (private communication).
[11] P. G. Radaelli, D. E. Cox, M. Marezio, S-W. Cheong, P. E. Schiffer, and A. P. Ramirez, Phys. Rev. Lett. **75**, 4488 (1995).
[12] J. M. DeTeresa, M. R. Ibarra, J. Blasco, J. Garcia, C. Marquina, P. A. Algarabel, Z. Arnold, K. Kamenev, C. Ritter, and R. von Helmolt, Phys. Rev. B **54**, 1187 (1996).
[13] A. C. Larson and R. B. Von Dreele, Los Alamos National Laboratory Report No. LA-UR-86-748 (unpublished).
[14] See AIP Document No. PAPS PRBMDO-58-063829 for 5 pages of tables of the atomic parameters and the relevant bond distances and angles. Order by PAPS number and journal reference from American Institute of Physics, Physics, Physics Auxiliary Publication Service, Carolyn Gehlbach, 500 Sunnyside Boulevard, Woodbury, NY 11797-2999. Fax: 516-576-2223, e-mail: paps@aip.org. The price is $1.50 for each microfiche (98 pages) or $5.00 for photocopies of up to 30 pages, and $0.15 for each additional page over 30 pages. Airmail additional. Make checks payable to the American Institute of Physics.
[15] J. A. M. Van Roosmalen and E. H. P. Cordfunke, J. Solid State Chem. **110**, 106 (1994).